giMLPs: Gate with Inhibition Mechanism in MLPs

Cheng Kang[1*], **Jindich Prokop**[1], **Lei Tong**[2], **Huiyu Zhou**[2], **Yong Hu**[3], **Daneil Novak**[1]

[1]Czech Technical University,[2]University of Leicester,[3]University of Hong Kong
{kangchen,prokojin,xnovakd1}@fel.cvut.cz,
{hz143,lt288}@leicester.ac.uk, yhud@hku.hk

arXiv:2208.00929v1 [cs.CL] 1 Aug 2022

Abstract

This paper presents a new model architecture, gate with inhibition MLP (giMLP). The gate with inhibition on CycleMLP (giCycleMLP) can produce the equal performance on ImageNet classification task, and it also improves the BERT, RoBERTa and DeBERTaV3 models depending on two novel techniques. The first is the gating MLP, where matrix multiplications between the MLP and the trunk Attention input in further adjust models' adaptation. The second is the inhibition which inhibits or enhances the branch adjustment, and with the inhibition levels increasing, it offers models stronger features restriction. We show that the giCycleMLP with a lower inhibition level can be competitive with original CycleMLP in terms of ImageNet classification accuracy. In addition, we also show through a comprehensive empirical study that these techniques significantly improve the performance on fine-tuning NLU downstream tasks. As for the gate with inhibition MLPs on DeBERTa (giDeBERTa) fine-tuning, we find it can achieve appealing results on most part of NLU tasks without any extra pretraining again. We also find that with the use of Gate With Inhibition, the activation function should have a short and smooth negative tail, with which the unimportant features or the features who have a negative effect on models can be moderately inhibited. The experiments on ImageNet and twelve language downstream tasks demonstrate the effectiveness of Gate With Inhibition, both for images classification and for enhancing the capacity of nature language fine-tuning without any extra pretraining. Code and models are available at: https://github.com/ChengKang520/gate-with-inhibition.

1 Introduction

As the history of computer vision and nature language processing demonstrate, respectively, Convolutional Neural Networks (CNNs) and Transformers based Language Models are the de-facto standards. Recently, many multi-layer perceptions (MLPs) based architectures have been proposed to process vision, for example, MLP-Mixer (Tolstikhin et al. 2021), ResMLP (Touvron et al. 2021a), gMLP (Liu et al. 2021a), CycleMLP (Chen et al. 2022). They used MLPs as the model trunk or as the branches with gate mechanism, and achieved surprisingly promising results on ImageNet (Deng et al. 2009) classification by building models solely on MLPs and skip connections without the self-attention layers. Moreover, for scaling language models, PaLM (Chowdhery et al. 2022) uses MLP branch on the Transformers, which means they add more weights on the language models to modify attention blocks. This is also the parallel layers in PaLM, and actually, when fine-tuning the downstream tasks, the SwiGLU activation function in PaLM acts like our gate with inhibition mechanism.

The major challenge for fine-tuning downstream NLU tasks is to select proper features in dense feature pools. That requires **(1)** pretraining on huge language datasets again, **(2)** branch pathways on features selection, and meanwhile, **(3)** capacity on discard or inhibit trivial features. In PaLM (Chowdhery et al. 2022), MLP branches are used to select trunk features, and the activation function SwiGLU is applied on gating MLPs and attention blocks. Thus, in this paper, we seek to answer this question: *can we improve language models by avoiding every time pretraining on huge language datasets, and improve Transformer models sparsity, and keep architecture efficiency, as well as maintaining higher prediction capacity?* As illustrated in Figure 1, we intentionally designed the inhibition level to make the activated features of language models not to be normally distributed after pretraining on huge language datasets. Through weakening the weights of irrelevant features during fine-tuning by removing some negative feature tails after using GELU or LeakyReLU activation functions, the distribution of the activated features tends to move forward to the specific downstream tasks with an incomplete Gaussian-like distribution of activated features. This is the reason why the distribution of activated features is not a complete Gaussian-like distribution after our gate with inhibition MLPs.

To address the first challenge, we directly apply several pretrained language models on fine-tuning downstream NLU tasks. As illustrated in Figure 2, for the second and the last issues, we construct a gating MLP branch architecture on Transformers to select features, meanwhile, propose an adaptive threshold as an inhibition level to adjust the gating branch weights. In this study, We proof the necessity of inhibition in gate MLPs for fine-tuning downstream nature language understanding (NLU) tasks by using some pretrained language models, and we also demonstrate the alternative on applying inhibition on vision applications of gate MLPs. Specifically,

*Corresponding Author.
Copyright © 2022, Association for the Advancement of Artificial Intelligence (www.aaai.org). All rights reserved.

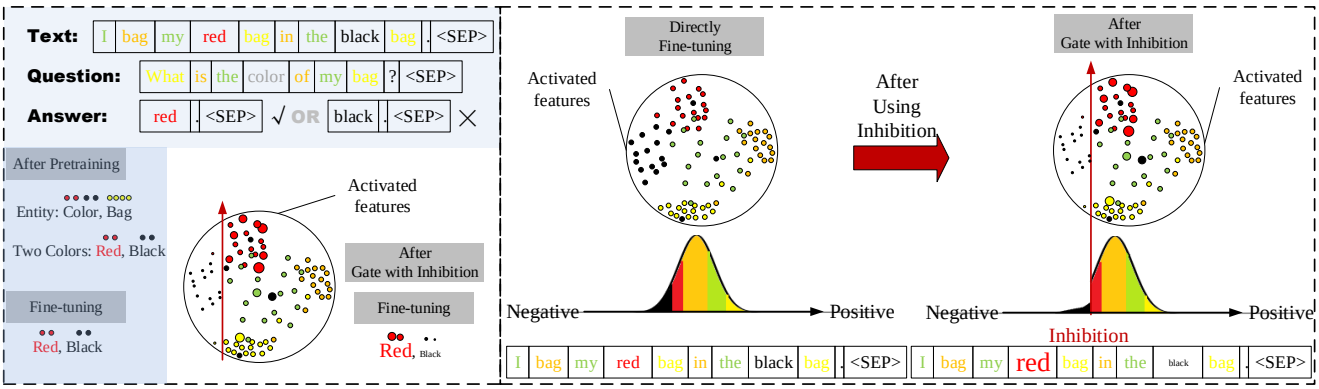

Figure 1: A schematic diagram of describing the giMLP and giTransformers for images classifying and downstream NLU tasks fine-tuning. If there is a text '| I bag my red bag in the black bag. |', and the question is '| What is the color of my bag? |', therefore, the answer should be '| red. |'. But for the entity extraction, there are two colors: red and black. Classical fine-tuning on downstream NLU tasks tends to weekly adjust models which finally make itself choose proper features or outputs very hard. Under gate with inhibition, after several epochs fine-tuning, the models both can learn an incomplete Gaussian-like distribution for activated features, with which the negative activated trunk features will be inhibited, and can further strengthen the important. That means the black related features eventually are inhibited, and on the contary, the red related features are enhanced.

we propose a gate with inhibition alternative to MLPs, which consists of the partially inhibited parameterization of channel and spatial projections. In addition, we insert this giMLP into the pretrained attention blocks of Transformers, and name this new Transformers as giTransformers.

We apply the gate with inhibition on BERT (Devlin et al. 2018) (giBERT), RoBERTa (Liu et al. 2019) (giRoBERTa) and DeBERTaV3 (He, Gao, and Chen 2021) (giDeBERTaV3) to downstream NLU tasks. These three gate with inhibition language models obtain stronger results on GLUE (Wang et al. 2018), as well as Question Answering: SQuAD v1.1 (Rajpurkar et al. 2016), SQuAD v2.0 (Rajpurkar, Jia, and Liang 2018) and SWAG (Zellers et al. 2018), and NER: CoNLL-2003. We also apply the gate with inhibition on CycelMLP-B1 (Chen et al. 2022) (giCycleMLP-B1) on ImageNet (Deng et al. 2009). Although the giCycleMLP-B1 always behinds CycleMLP-B1 in the early training stage, the giCycleMLP-B1 finally achieves equal and comparable performance with CycleMLP-B1 (Chen et al. 2022).

The contributions of this paper are as follows: **(1)** We take the first attempt to fine-tune downstream NLU tasks without pretraining new language models on huge language datasets, and achieve stronger results. **(2)** We propose the gate with inhibition MLP, a new MLP-like operator, which is computational friendly to cope with features selection and trivial features inhibition. **(3)** Image classification experiment on ImageNet demonstrates that giMLP is comparable to CNNs on dense predictions. **(4)** Extensive experiments on various tasks (e.g., GLUE, SQuAD v1.1, SQuAD v2.0, SWAG and NER: CoNLL-2003) demonstrate that giTransformers outperforms existing Transformers language models and sometimes is better than Transformers on downstream NLU tasks fine-tuning.

2 Background And Related Works

2.1 Language Models And Scaling

By stacking Transformer blocks,Transformer-based language models have been served as the standard architecture (Vaswani et al. 2017). Exploring the mechanism of scaling Transformer (by scaling model size, dataset size, model shape, context length and batch size), which was encouraged by the scaling law (Kaplan et al. 2020), has accelerated the capacity of various language models, such as masked or autoregressive language modeling (Devlin et al. 2018; Radford et al. 2019). From BERT (Devlin et al. 2018; Radford et al. 2019) by jointly conditioning on both left and right context, to the Megatron-Turing-530B (Brown et al. 2020; Shoeybi et al. 2019; Raffel et al. 2019; Smith et al. 2022) by constructing transformer-based language model with 530 billion parameters, to RoBERTa (Liu et al. 2019) with designed choices and alternatives, to ALBERT (Lan et al. 2019) which used scaling mechanism, to SqueezeBERT (Iandola et al. 2020) with grouped convolutions, to DeBERTa (He et al. 2020; He, Gao, and Chen 2021) by a virtual adversarial training method, to sparse Switch-Transformer-1.6T (Fedus, Zoph, and Shazeer 2021) with mixture, and to Swin-Transformer (Liu et al. 2021d,c) which simplifies and improves over mixture of models, the capacity of language models have been improved dramatically by more than 1,000 times during these years.

To encode position information of words, existing approaches add a positional bias to each input word embedding so that each input word is represented by a vector whose value depends on its content and position. The positional bias can be implemented using absolute position embedding (Vaswani et al. 2017; Devlin et al. 2018; Radford et al. 2019) or relative position embedding (Yang et al. 2019). It has been shown that relative position representations are more effective for

natural language understanding and generation tasks (Dai et al. 2019; Shaw, Uszkoreit, and Vaswani 2018).

Study on bias terms in NLP, the relative position bias method proved beneficial (Raffel et al. 2019), compared to the absolute position embedding used in the original Transformer (Vaswani et al. 2017). In computer vision, the relative positional bias method is more commonly used (Liu et al. 2021d; Hu et al. 2019; Yang et al. 2021), probably because the spatial relationships of visual signals play a more important role in visual modeling. A common practice is to directly learn the bias values as model weights. There are also a few works particularly study how to set and learn the bias terms (Ke, He, and Liu 2020; Wu et al. 2021).

Taking single-head attention as an example, the self-attention operation with bias can be formulated as (Vaswani et al. 2017; Smith et al. 2022; He et al. 2020; Liu et al. 2021d):

$$Q = HW_q + bias_q, K = HW_k + bias_k, V = HW_v + bias_v \tag{1}$$

$$A = \frac{QK^T}{\sqrt{D}} \tag{2}$$

$$H_o = softmax(A + bias_a)V \tag{3}$$

where $H \in R^{M\times D}$ represents the input hidden vectors. $H_o \in R^{M\times D}$ is the output of self-attention. $Q, K, V \in R^{M\times D}$ are the $Query, Key$ and $Value$ matrices. $W_q, W_k, W_v \in R^{M\times D}$ are the projection matrices. $A \in R^{M\times D}$ is the attention matrix. M is the length of the input sequence. $bias_a, bias_q, bias_k, bias_v \in R^{M\times M}$ are the relative position bias term for each head, and D is the dimension of hidden states.

2.2 Gating Unit In Spatial Dimension

The overall formulation of Gated Linear Units (GLUs) (Shazeer 2020; Wu et al. 2019; Liu et al. 2021a) could be summarized as linear projections:

$$L_{w,bias}(X) = W_1X + bias_1 \tag{4}$$

$$L_g(X) = GELU(W_g[GELU(W_2X + bias_2) + bias_g]) \tag{5}$$

$$Z_g(X) = L_g(X) \odot [L_{w,bias}(X) + 1] \tag{6}$$

where GELU (Hendrycks and Gimpel 2016) is an activation function. $X \in R^{M\times D}$, $W_1, W_2, W_g \in R^{M\times M}$ are matrices for whose size is the same as the sequence length, $bias_1, bias_2, bias_g \in R^{M\times M}$ refer biases. $L_{w,bias}$ is the projection of trunk layers, $L_g(X)$ is the projection of gate branch layers, and $Z_g(X)$ is the output of linear gating.

A key distinction is that our gating is computed based on a projection over the spatial (cross-token) dimension rather than the channel (hidden) dimension. SGU (Spatial Gating Unit) is also related to Squeeze-and-Excite (SE) blocks (Hu, Shen, and Sun 2018) in terms of element-wise multiplication. However, different from SE blocks, SGU does not contain cross-channel projections at all, nor does it enforce permutation invariance (a key feature for content-based attentive modules) due to its static parameterization for the spatial transformation. The spatial projection in SGU could in theory learn to express superficial depthwise convolutions—unlike typical depthwise convolutions with channel-specific filters, SGU learns only a single transformation shared across channels. Finally, we note SGUs offer an alternative mechanism to capture high-order relationships other than self-attention.

2.3 Threshold And Inhibition

Threshold has been mostly used in Deep Spiking Neural Networks (SNNs) (Tavanaei et al. 2019; Sengupta et al. 2019; Lobo et al. 2020). The threshold value is very significant for the correct operation of SNNs because a high threshold will prevent the neuron from firing ("dead-neuron" problem), and a lower threshold will lead to excessive firing, affecting the ability of the neuron to differentiate between two input patterns (Rathi and Roy 2021). The firing thresholds are also fixed (Lee et al. 2020) or selected based on some heuristics (Sengupta et al. 2019; Rueckauer et al. 2017). In (Sengupta et al. 2019), the threshold was selected as the maximum preactivation of each layer, whereas (Rueckauer et al. 2017) selected a certain percentile of the preactivation distribution as the threshold. Some recent works employ leak/threshold optimization, but their application is limited to simple datasets (Fang et al. 2021; Yin, Corradi, and Bohté 2020). Most of these articles applied threshold to SNNs, but they are facing the challenge proposing improper methods of selecting the membrane leak and the threshold. However, according to our best knowledge, there is no example of applying inhibition in CNNs and Transformers.

3 Gate With Inhibition

Our architecture, gate with inhibition, consists of a stack of gate blocks with an additional threshold. Gate blocks can select which features should be focused on, and inhibition can control the opening level of the gate. In this article, in order to reveal the influence of different inhibition levels on MLPs and Transformers, we set the hyperparameter inhibition percentile Inh_p as 0%, 10%, 30%, 90%. In Figure 1, there is an example which can explain how gate with inhibition works on images classifying and downstream NLU tasks fine-tuning.

3.1 Gate Transformers With Inhibition

Previous attempts have revealed that the self-attention probability in Transformers has a sparse distribution, and have proposed several selection strategies. The Sparse Transformer](Child et al. 2019) uses separated spatial correlation to incorporate both the row outputs and column inputs, and the LogSparse Transformer (Li et al.) designs the cyclical pattern in self-attention and forces each cell to attend to its previous one by an exponential step size.

Notation. We denote input hidden vectors as $H \in R^{M\times D}$ and the output of self-attention as $\bar{H}_o \in R^{M\times D}$. $W_{kg}, W_{ki}, W_{qg}, W_{qi}, W_v \in R^{M\times D}$ are the projection matrices. M is the length of the input sequence and D is the dimension of hidden states. See Appendix Algorithm2.

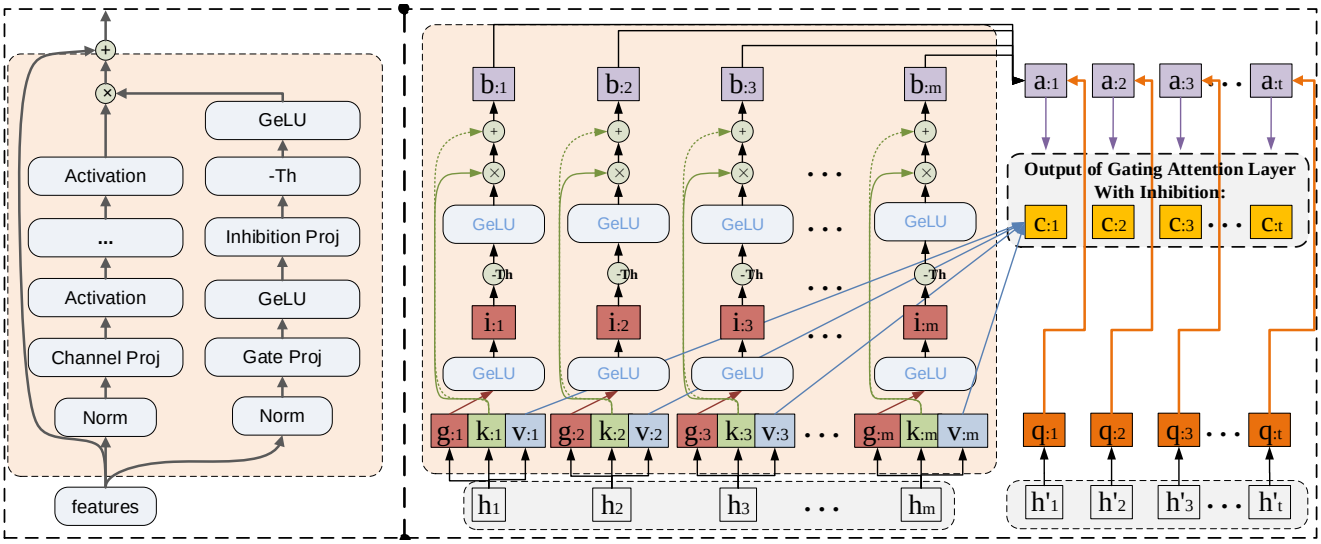

Figure 2: The Architecture of Gate With Inhibition in MLPs and Transformers' Key side.

Table 1: Comparison results on fine-tuning the GLUE development set, SQuAD v1.1, SQuAD v2.0, SWAG and NER. (gi+ means we embed the gate with inhibition mechanism into BERT(1*), RoBERTa(2*) and DeBERTa(3*). The values after giBERT, giRoBERTa and giDeBERTa are inhibition levels. Note that missing results in literature are signified by "-").

	Model **#Train**	**GLUE**									**SQuAD v1.1**	**SQuAD v2.0**	**SWAG**	**NER**
	(Large)	CoLA Mcc 8.5k	QQP Acc 364k	MNLI-m/mm Acc 393k	SST-2 Acc 67k	STS-B Corr 7k	QNLI Acc 108k	RTE Acc 2.5k	MRPC Acc 3.7k	Avg.	F1/EM 87.6k	F1/EM 130.3k	Acc 73.5k	F1 14987
	BERT (Devlin et al. 2018)	60.6	91.3	86.6/-	93.2	90.0	92.3	70.4	88.0	84.5	90.9/84.5	81.8/79.0	88.6	92.8
	RoBERTa (Liu et al. 2019)	68.0	92.2	90.2/90.2	96.4	92.4	93.9	86.6	90.9	88.82	94.5/88.9	89.4/86.5	89.9	93.4
	XLNet (Yang et al. 2019)	69.0	92.3	90.8/90.8	97.0	92.5	94.9	85.9	90.8	89.15	94.5/89.0	88.8/86.1	-	-
	ALBERTA (Lan et al. 2019)	68.7	92.0	90.4/-	96.8	92.7	95.2	88.1	90.2	89.26	94.8/89.2	89.9/87.2	84.9/81.8	-
	ELECTRA (Clark et al. 2020)	69.1	92.4	90.9/-	96.9	92.6	95.0	88.0	90.8	89.46	94.9/89.7	90.6/88.0	-	-
	DeBERTaV2 (He et al. 2020)	70.5	92.3	91.1/91.1	96.8	92.8	95.2	88.3	91.9	90.00	**95.5/90.1**	90.7/88.0	90.8	93.8
	DeBERTaV3 (He, Gao, and Chen 2021)	75.3	93.0	**91.8/91.9**	96.9	92.7	95.4	90.3	92.7	**91.37**	-	91.5/89.0	93.4	93.9
	BERT(fine-tune)	64.0	91.3	86.2/-	93.8	88.9	92.6	***71.4***	86.6	***84.35***	91.3/84.5	81.7/78.4	86.5	95.4
	giBERT(0)	65.5	91.5	86.6/-	93.9	88.7	92.5	66.4	85.0	83.76	91.1/84.3	81.6/78.9	86.6	95.2
1*	giBERT(0.1)	65.8	91.4	86.5/-	93.5	88.9	92.4	70.1	83.1	83.96	91.1/84.4	81.3/78.5	86.5	95.6
	giBERT(0.3)	***65.9***	***91.5***	86.3/-	***94.4***	89.0	***92.7***	69.0	84.8	84.19	91.1/84.4	81.4/78.1	***86.7***	***95.6***
	giBERT(0.9)	64.3	91.4	86.3/-	93.3	88.3	92.4	71.1	84.3	83.70	***91.3/84.6***	***81.8/79.1***	86.7	95.6
	RoBERTa(fine-tune)	68.1	92.2	90.2/90.2	96.3	92.3	93.9	86.6	90.9	88.56	94.1/88.4	88.9/86.0	89.9	93.4
	giRoBERTa(0)	64.1	92.2	90.2/90.2	95.8	92.0	94.1	85.2	89.0	87.81	93.9/88.4	88.3/84.7	88.3	96.8
2*	giRoBERTa(0.1)	65.5	92.0	89.5/89.5	95.6	92.4	94.4	83.4	***91.7***	88.05	94.1/88.8	88.5/85.5	88.4	96.5
	giRoBERTa(0.3)	***68.8***	92.2	90.1/90.1	96.4	91.6	***94.5***	84.9	91.0	88.68	94.2/88.8	88.7/85.3	89.6	96.7
	giRoBERTa(0.9)	67.5	92.1	89.6/89.6	95.8	91.6	94.1	85.2	89.7	88.20	***94.7/89.2***	89.1/86.3	89.9	96.9
	DeBERTaV3(fine-tune)	72.3	93.0	91.0/90.9	96.2	92.6	95.4	90.3	90.7	90.19	95.4/89.8	91.5/89.0	93.3	96.8
	giDeBERTaV3(0)	73.2	93.1	90.9/90.9	96.6	93.2	95.5	90.3	91.4	90.65	95.2/89.7	90.8/88.5	91.9	96.8
3*	giDeBERTaV3(0.1)	**76.5**	**93.2**	90.8/90.8	96.2	**93.2**	**96.0**	90.0	92.3	91.25	95.3/89.9	91.2/88.7	93.3	96.8
	giDeBERTaV3(0.3)	74.0	93.0	91.1/91.1	96.9	93.2	95.8	**90.7**	**93.1**	90.99	95.4/89.9	91.1/88.4	**93.5**	**97.1**
	giDeBERTaV3(0.9)	72.8	93.0	90.9/90.9	96.2	92.6	95.5	89.5	90.7	90.19	95.4/90.0	**91.6/89.0**	93.3	96.8

Motivation. The motivation of giTransformers is to assemble a flexible gate with an adjustable quantized inhibition to cope with downstream language tasks. In addition, it should be able to automatically learn to rarefy tense features without sparsity settings. Under transfer learning, the pretrained language models can provide features for nature language downstream tasks, but the Gate With Inhibition layers will learn to enhance, maintain and inhibit the provided features, which finally can fit specific downstream language tasks. As illustrated in the right panel of Figure2, the Gate With Inhibition layers on both Key and Query sides can bring fully potential work on Value matrices, as Key matrices project the importance of hidden inputs, and Query matrices represent the correlation-like relationship on hidden inputs and outputs. We formulate the linear gate with inhibition layer in Transformers as:

$$G_k = GELU(HW_{kg} + bias_{kg}) \tag{7}$$

$$I_k = GELU(G_k W_{ki} + bias_{ki} - Th_k) \tag{8}$$

$$G_q = GELU(HW_{qg} + bias_{qg}) \tag{9}$$

$$I_q = GELU(G_q W_{qi} + bias_{qi} - Th_q) \tag{10}$$

$$V = HW_v + bias_v, K = HW_k + bias_k, Q = HW_q + bias_q \tag{11}$$

$$B_k = K + I_k, B_q = Q + I_q, \bar{A}_{kq} = \frac{B_q B_k^T}{\sqrt{d}} \tag{12}$$

$$\bar{H}_o = softmax(\bar{A}_{kq} + bias_{\bar{a}})V \tag{13}$$

where $G_k, I_k \in R^{M\times D}$ are the $Gate$ and $Inhibition$ matrices in Key side, $G_q, I_q \in R^{M\times D}$ are the $Gate$ and $Inhibition$ matrices in $Query$ side, and $V \in R^{M\times D}$ is the $Value$ matrix. $B_k, B_q \in R^{M\times D}$ are respectively Key and $Query$ matrices with Gate With Inhibition. $\bar{A}_{kq} \in R^{M\times D}$ is the attention matrix with Gate With Inhibition. $bias_{kg}, bias_{ki}, bias_{qg}, bias_{qi}, bias_v, bias_{\bar{a}} \in R^{M\times M}$ are the relative position bias term for each head. Th_k is the product of $max(G_k W_{ki}) \times percentile$. Th_q is the product of $max(G_q W_{qi}) \times Inh_p$.

4 Masked Language Modeling On giBERTs

Our submission depends only on single-task finetuning. This section reports BERT, RoBERTa and DeBERTaV3 all with Gate With Inhibition results on various NLU tasks. Following and comparing with previous studies of pretrained language models, we report results using large models. We use 8 $\times$ NVIDIA Tesla A100 with 40GB graphic memory to fine-tune the models. Refer to Appendix A.3 Table 3 for the detailed hyperparamters. Here we compare our giTransformers models with recent attentive models based on vanilla Transformers, including BERT (Devlin et al. 2018), RoBERTa (Liu et al. 2019), DeBERTa (He et al. 2020) and DeBERTaV3 (He, Gao, and Chen 2021). Language models based on Transformers tend to drastically overfit the training data, and this finally would bring a negative effect on downstream fine-tuning. Redundant features induced by pretraining will interfere language models' performance, especially on small tasks. We therefore apply a similar MLP architecture (as the one used in gMLP (Liu et al. 2021b)) with inhibition to avoid extensive tuning. After inserting gate with inhibition into BERT, RoBERTa and DeBERTa, we summarize the results on eight NLU tasks of GLUE (Wang et al. 2018), as well as Question Answering: SQuAD v1.1 (Rajpurkar et al. 2016), SQuAD v2.0 (Rajpurkar, Jia, and Liang 2018) and SWAG (Zellers et al. 2018), and NER: CoNLL-2003 in Table 1, and compare them with current SOTA result, from $BERT_{large}$(Devlin et al. 2018) to $RoBERTa_{large}$(Liu et al. 2019), $ALBERT_{large}$(Lan et al. 2019), $XLNet_{large}$(Yang et al. 2019), $ELECTRA_{large}$(Clark et al. 2020), $Megatron_{336M}$(Shoeybi et al. 2019), $DeBERTa_{large}$(He et al. 2020), $DeBERTaV3_{large}$(He, Gao, and Chen 2021). Meanwhile, giDeBERTaV3 outperforms original DeBERTaV3 in nine out of twelve tasks. Particularly, the improvements on CoLA (1.2% over original DeBERTaV3 when In_p is 10%), QQP (0.2% over original DeBERTaV3 when In_p is 10%), STS-B (0.5% over original DeBERTaV3 when In_p is 10%), QNLI (0.6% over original DeBERTaV3 when In_p is 10%), RTE (0.4% over original DeBERTaV3 when In_p is 30%) and MRPC (0.4% over original DeBERTaV3 when In_p is 30%) are significant. The giDeBERTaV3 also outperforms other SOTA, i.e., $ELECTRA_{large}$, $Megatron_{336M}$ and $XLNet_{large}$.

4.1 Ablation: The Importance Of Gating With Inhibition For BERT's Fine-tuning

Our setting for giBERT large model is similar to the input/output protocol for BERT finetuning (Devlin et al. 2018).

In Table 1 (**1***), giBERT without an extra pretraining outperforms original BERT in four out of eight tasks, and only two weaker than BERT with extra 5 epochs fine-tuning. Particularly, when the inhibition percentile is 10%, the great improvements on CoLA (5.3% over original BERT and 1.9% over original BERT with extra 5 epochs fine-tuning), SST-2 (1.2% over original BERT and 0.6% over original BERT with extra 5 epochs fine-tuning), as well as little improvement on QQP and QNLI (0.2% over both original BERT and original BERT with extra 5 epochs fine-tuning) and QNLI (0.2% over original BERT and 0.1% over original BERT with extra 5 epochs fine-tuning). The BERT inserted with Gate With Inhibition without an extra pretraining could not achieve better results on STS-B, RTE and MRPC, and the inferred reason is that the additive weights on giBERT need more training steps, which means that the obvious shortage of giBERT is fine-tuning small downstream tasks.

Only when the inhibition percentile is 90%, the giBERT can achieve weak advantages on SQuAD v1.1, SQuAD v2.0, SWAG and NER, although the giBERT is $15\% \sim 30\%$ (depends on models' original size) bigger than the original BERT, which means that we sacrifice more $15\% \sim 30\%$ weights to achieve a better performance.

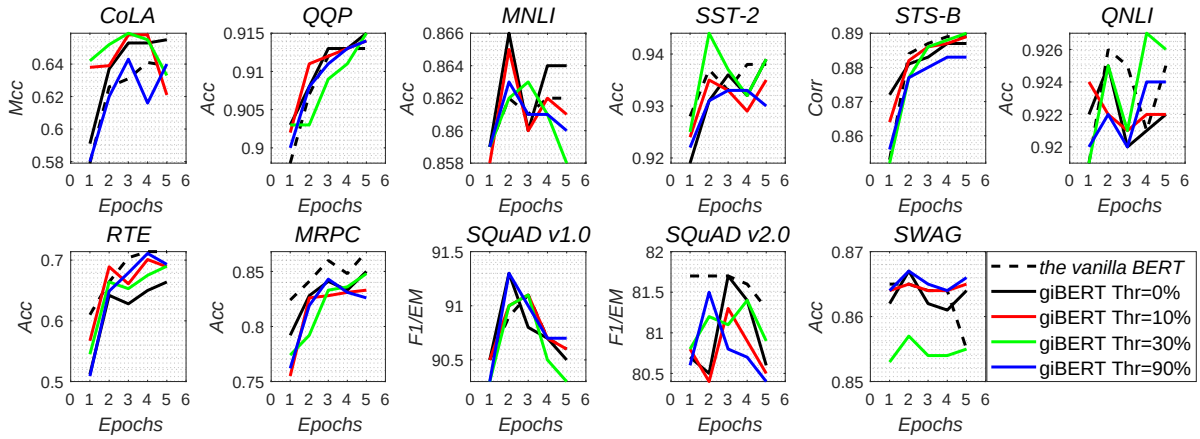

Figure 3: Plots of corresponding metrics according to the number of epochs on the validation split of GLUE, SQuAD v1.1, SQuAD v2.0 and SWAG.

4.2 Ablation: The Gating With Inhibition On RoBERTa's And DeBERTa's Fine-tuning

Our setting for giRoBERTa and giDeBERTa large models are respectively similar to the input/output protocol for RoBERTa (Liu et al. 2019) and DeBERTaV3 (He, Gao, and Chen 2021) finetuning. We summarized the comparison results on these twelve NLU tasks in Table 1 (**2*** and **3***), in terms of fine-tuning the architecture of inserting gate with inhibition into original RoBERTa and DeBERTa.

In Table In Table 1 (**2*** and **3***), giRoBERTa without an extra pretraining outperforms original RoBERTa on five out of twelve tasks, produces the equal performance on other five out of twelve tasks, and only two weaker than RoBERTa with extra 10 epochs fine-tuning. Particularly, when the inhibition percentile is 30%, the great improvements on CoLA (0.8% over original RoBERTa and 0.7% over original RoBERTa with extra 10 epochs fine-tuning), MRPC (0.8% over original RoBERTa and 2.5% over original RoBERTa with extra 10 epochs fine-tuning), QNLI (0.6% over both original RoBERTa and original RoBERTa with extra 10 epochs fine-tuning), as well as little improvement on SQuAD v1.1 and NER. We infer the reason why the giRoBERTa architecture without an extra pretraining could not achieve better results on SQuAD v1.1 and RTE is that, RoBERTa pretrained over 160GB of text with larger mini-batches and a larger byte-level Byte-Pair Encoding (Sennrich, Haddow, and Birch 2015), with which RoBERTa finally gained a robust model with the capacity of handling the large and wide vocabularies (Liu et al. 2019), and it also needs more training steps to fine-tune small downstream tasks.

The giDeBERTav3 without an extra pretraining outperforms original DeBERTaV3 on nine out of twelve tasks, produces the equal performance on only one task, and two weaker than DeBERTaV3 with extra 10 epochs fine-tuning. Particularly, when the inhibition percentile is 10% or 30%, the great improvements on CoLA (1.2% over original DeBERTaV3 and 4.2% over original DeBERTaV3 with extra 10 epochs fine-tuning), STS-B (0.5% over original DeBERTaV3 and 0.6% over original DeBERTaV3 with extra 10 epochs fine-tuning), QNLI (0.6% over both original RoBERTa and original RoBERTa with extra 10 epochs fine-tuning), RTE (0.4% over both original RoBERTa and original RoBERTa with extra 10 epochs fine-tuning), MRPC (0.4% over original DeBERTaV3 and 2.4% over original DeBERTaV3 with extra 10 epochs fine-tuning), as well as little improvement on QQP, SQuAD v2.0 and SWAG when the inhibition percentile is 30% or 90%.

There are content vector and position vector inside the DeBERTa architecture, and its attention weights among words are computed using disentangled matrices respectively based on their contents and relative positions (He, Gao, and Chen 2021). These two vectors make a stronger contextual relationship in input word vectors, and with Gate With Inhibition, giDeBERTa has the ability to automatically select the content and position with branch scaling extra weights. After that, during fine-tuning downstream tasks, this gate with inhibition block can act as a sparse setting layer with which can offer positive weight to enhance important and significant connections, during selecting and connecting features in highly dense feature pools.

5 Conclusion

In this paper, a new model architecture gate with inhibition is presented. The giCycleMLP, which is assembled with gate andinhibition, can produce the equal performance on ImageNet classification task. This gate with inhibition mechanism also improves the BERT, RoBERTa and DeBERTaV3 models using two novel techniques. The first is the gating MLP, where matrix multiplications between the MLP and the trunk or the Attention input in further adjust models' adaptation. The second is the inhibition which inhibits or enhances the branch adjustment, and with the inhibition levels increasing, it offers models stronger features restriction.

We show that the giCycleMLP with a lower inhibition level

can be competitive with original CycleMLP in terms of ImageNet classification accuracy, and we also show through a comprehensive empirical study that these techniques significantly improve the performance of NLU downstream tasks. As for giDeBERTa finetuning, we find it can achieve appealing results on most part of NLU tasks without an extra pretraining. We also find that with the use of Gate With Inhibition, the activation function should have a short and smooth negative tail, with which the unimportant features or the features who have a negative effect on models can be moderately inhibited. The experiments on training ImageNet and fine-tuning these downstream tasks demonstrated the effectiveness of Gate With Inhibition, either for images classification, or for enhancing the capacity of nature language fine-tuning without an extra pretraining.

6 Acknowledgements

Cheng Kang, Jindich Prokop and Daneil Novak are supported by the Czech Technical University in Prague (grant number: $SGS19/171/OHK3/3T/13$) and the Research Centre for Informatics (grant number: $CZ.02.1.01/0.0/16019/0000765$). We thank Yong Hu, Huiyu Zhou and Daneil Novak for proofreading the paper and providing insightful comments. We also thank Jindich Prokop, Lei Tong for their help with large-scale model training. We also thank the anonymous reviewers for valuable discussions.

References

Agarap, A. F. 2018. Deep learning using rectified linear units (relu). *arXiv preprint arXiv:1803.08375*.

Borg-Graham, L. J.; Monier, C.; and Fregnac, Y. 1998. Visual input evokes transient and strong shunting inhibition in visual cortical neurons. *Nature*, 393(6683): 369–373.

Brown, T.; Mann, B.; Ryder, N.; Subbiah, M.; Kaplan, J. D.; Dhariwal, P.; Neelakantan, A.; Shyam, P.; Sastry, G.; Askell, A.; et al. 2020. Language models are few-shot learners. *Advances in neural information processing systems*, 33: 1877–1901.

Chen, S.; Xie, E.; GE, C.; Chen, R.; Liang, D.; and Luo, P. 2022. CycleMLP: A MLP-like Architecture for Dense Prediction. In *International Conference on Learning Representations*.

Child, R.; Gray, S.; Radford, A.; and Sutskever, I. 2019. Generating long sequences with sparse transformers. *arXiv preprint arXiv:1904.10509*.

Chowdhery, A.; Narang, S.; Devlin, J.; Bosma, M.; Mishra, G.; Roberts, A.; Barham, P.; Chung, H. W.; Sutton, C.; Gehrmann, S.; et al. 2022. Palm: Scaling language modeling with pathways. *arXiv preprint arXiv:2204.02311*.

Clark, K.; Luong, M.-T.; Le, Q. V.; and Manning, C. D. 2020. Electra: Pre-training text encoders as discriminators rather than generators. *arXiv preprint arXiv:2003.10555*.

Clevert, D.-A.; Unterthiner, T.; and Hochreiter, S. 2015. Fast and accurate deep network learning by exponential linear units (elus). *arXiv preprint arXiv:1511.07289*.

Cubuk, E. D.; Zoph, B.; Shlens, J.; and Le, Q. V. 2020. Randaugment: Practical automated data augmentation with a reduced search space. In *Proceedings of the IEEE/CVF Conference on Computer Vision and Pattern Recognition Workshops*, 702–703.

Dai, Z.; Yang, Z.; Yang, Y.; Carbonell, J.; Le, Q. V.; and Salakhutdinov, R. 2019. Transformer-xl: Attentive language models beyond a fixed-length context. *arXiv preprint arXiv:1901.02860*.

Deng, J.; Dong, W.; Socher, R.; Li, L.-J.; Li, K.; and Fei-Fei, L. 2009. Imagenet: A large-scale hierarchical image database. In *2009 IEEE conference on computer vision and pattern recognition*, 248–255. Ieee.

Devlin, J.; Chang, M.-W.; Lee, K.; and Toutanova, K. 2018. Bert: Pre-training of deep bidirectional transformers for language understanding. *arXiv preprint arXiv:1810.04805*.

Fang, W.; Yu, Z.; Chen, Y.; Masquelier, T.; Huang, T.; and Tian, Y. 2021. Incorporating learnable membrane time constant to enhance learning of spiking neural networks. In *Proceedings of the IEEE/CVF International Conference on Computer Vision*, 2661–2671.

Fedus, W.; Zoph, B.; and Shazeer, N. 2021. Switch transformers: Scaling to trillion parameter models with simple and efficient sparsity. *arXiv preprint arXiv:2101.03961*.

He, K.; Zhang, X.; Ren, S.; and Sun, J. 2015. Delving deep into rectifiers: Surpassing human-level performance on imagenet classification. In *Proceedings of the IEEE international conference on computer vision*, 1026–1034.

He, P.; Gao, J.; and Chen, W. 2021. Debertav3: Improving deberta using electra-style pre-training with gradient-disentangled embedding sharing. *arXiv preprint arXiv:2111.09543*.

He, P.; Liu, X.; Gao, J.; and Chen, W. 2020. Deberta: Decoding-enhanced bert with disentangled attention. *arXiv preprint arXiv:2006.03654*.

Hendrycks, D.; and Gimpel, K. 2016. Bridging nonlinearities and stochastic regularizers with gaussian error linear units.

Hu, H.; Zhang, Z.; Xie, Z.; and Lin, S. 2019. Local relation networks for image recognition. In *Proceedings of the IEEE/CVF International Conference on Computer Vision*, 3464–3473.

Hu, J.; Shen, L.; and Sun, G. 2018. Squeeze-and-excitation networks. In *Proceedings of the IEEE conference on computer vision and pattern recognition*, 7132–7141.

Huang, G.; Sun, Y.; Liu, Z.; Sedra, D.; and Weinberger, K. Q. 2016. Deep networks with stochastic depth. In *European conference on computer vision*, 646–661. Springer.

Huang, W.; Ke, Y.; Zhu, J.; Liu, S.; Cong, J.; Ye, H.; Guo, Y.; Wang, K.; Zhang, Z.; Meng, W.; et al. 2021. TRESK channel contributes to depolarization-induced shunting inhibition and modulates epileptic seizures. *Cell Reports*, 36(3): 109404.

Iandola, F. N.; Shaw, A. E.; Krishna, R.; and Keutzer, K. W. 2020. SqueezeBERT: What can computer vision teach NLP about efficient neural networks? *arXiv preprint arXiv:2006.11316*.

Joshi, M.; Chen, D.; Liu, Y.; Weld, D. S.; Zettlemoyer, L.; and Levy, O. 2020. Spanbert: Improving pre-training by representing and predicting spans. *Transactions of the Association for Computational Linguistics*, 8: 64–77.

Kaplan, J.; McCandlish, S.; Henighan, T.; Brown, T. B.; Chess, B.; Child, R.; Gray, S.; Radford, A.; Wu, J.; and Amodei, D. 2020. Scaling laws for neural language models. *arXiv preprint arXiv:2001.08361*.

Ke, G.; He, D.; and Liu, T.-Y. 2020. Rethinking positional encoding in language pre-training. *arXiv preprint arXiv:2006.15595*.

Kingma, D. P.; and Ba, J. 2014. Adam: A method for stochastic optimization. *arXiv preprint arXiv:1412.6980*.

Klambauer, G.; Unterthiner, T.; Mayr, A.; and Hochreiter, S. 2017. Self-normalizing neural networks. *Advances in neural information processing systems*, 30.

Lan, Z.; Chen, M.; Goodman, S.; Gimpel, K.; Sharma, P.; and Soricut, R. 2019. Albert: A lite bert for self-supervised learning of language representations. *arXiv preprint arXiv:1909.11942*.

Lee, C.; Sarwar, S. S.; Panda, P.; Srinivasan, G.; and Roy, K. 2020. Enabling spike-based backpropagation for training deep neural network architectures. *Frontiers in neuroscience*, 119.

Li, S.; Jin, X.; Xuan, Y.; Zhou, X.; Chen, W.; Wang, Y.-X.; and Yan, X. ???? Enhancing the Locality and Breaking the Memory Bottleneck of Transformer on Time Series Forecasting. In Wallach, H.; Larochelle, H.; Beygelzimer, A.; d'Alché-Buc, F.; Fox, E.; and Garnett, R., eds., *Advances in Neural Information Processing Systems*. Curran Associates, Inc.

Liu, H.; Dai, Z.; So, D.; and Le, Q. V. 2021a. Pay attention to mlps. *Advances in Neural Information Processing Systems*, 34: 9204–9215.

Liu, H.; Dai, Z.; So, D.; and Le, Q. V. 2021b. Pay Attention to MLPs. In Ranzato, M.; Beygelzimer, A.; Dauphin, Y.; Liang, P.; and Vaughan, J. W., eds., *Advances in Neural Information Processing Systems*, volume 34, 9204–9215. Curran Associates, Inc.

Liu, Y.; Ott, M.; Goyal, N.; Du, J.; Joshi, M.; Chen, D.; Levy, O.; Lewis, M.; Zettlemoyer, L.; and Stoyanov, V. 2019. Roberta: A robustly optimized bert pretraining approach. *arXiv preprint arXiv:1907.11692*.

Liu, Z.; Hu, H.; Lin, Y.; Yao, Z.; Xie, Z.; Wei, Y.; Ning, J.; Cao, Y.; Zhang, Z.; Dong, L.; et al. 2021c. Swin Transformer V2: Scaling Up Capacity and Resolution. *arXiv preprint arXiv:2111.09883*.

Liu, Z.; Lin, Y.; Cao, Y.; Hu, H.; Wei, Y.; Zhang, Z.; Lin, S.; and Guo, B. 2021d. Swin transformer: Hierarchical vision transformer using shifted windows. In *Proceedings of the IEEE/CVF International Conference on Computer Vision*, 10012–10022.

Lobo, J. L.; Del Ser, J.; Bifet, A.; and Kasabov, N. 2020. Spiking neural networks and online learning: An overview and perspectives. *Neural Networks*, 121: 88–100.

Loshchilov, I.; and Hutter, F. 2017. Decoupled weight decay regularization. *arXiv preprint arXiv:1711.05101*.

Paszke, A.; Gross, S.; Massa, F.; Lerer, A.; Bradbury, J.; Chanan, G.; Killeen, T.; Lin, Z.; Gimelshein, N.; Antiga, L.; et al. 2019. Pytorch: An imperative style, high-performance deep learning library. *Advances in neural information processing systems*, 32.

Radford, A.; Wu, J.; Child, R.; Luan, D.; Amodei, D.; Sutskever, I.; et al. 2019. Language models are unsupervised multitask learners. *OpenAI blog*, 1(8): 9.

Raffel, C.; Shazeer, N.; Roberts, A.; Lee, K.; Narang, S.; Matena, M.; Zhou, Y.; Li, W.; and Liu, P. J. 2019. Exploring the limits of transfer learning with a unified text-to-text transformer. *arXiv preprint arXiv:1910.10683*.

Rajpurkar, P.; Jia, R.; and Liang, P. 2018. Know what you don't know: Unanswerable questions for SQuAD. *arXiv preprint arXiv:1806.03822*.

Rajpurkar, P.; Zhang, J.; Lopyrev, K.; and Liang, P. 2016. Squad: 100,000+ questions for machine comprehension of text. *arXiv preprint arXiv:1606.05250*.

Ramachandran, P.; Zoph, B.; and Le, Q. V. 2017. Searching for activation functions. *arXiv preprint arXiv:1710.05941*.

Rao, Y.; Zhao, W.; Zhu, Z.; Lu, J.; and Zhou, J. 2021. Global Filter Networks for Image Classification. In Ranzato, M.; Beygelzimer, A.; Dauphin, Y.; Liang, P.; and Vaughan, J. W., eds., *Advances in Neural Information Processing Systems*, volume 34, 980–993. Curran Associates, Inc.

Rathi, N.; and Roy, K. 2021. Diet-snn: A low-latency spiking neural network with direct input encoding and leakage and threshold optimization. *IEEE Transactions on Neural Networks and Learning Systems*.

Rueckauer, B.; Lungu, I.-A.; Hu, Y.; Pfeiffer, M.; and Liu, S.-C. 2017. Conversion of continuous-valued deep networks to efficient event-driven networks for image classification. *Frontiers in neuroscience*, 11: 682.

Sengupta, A.; Ye, Y.; Wang, R.; Liu, C.; and Roy, K. 2019. Going deeper in spiking neural networks: VGG and residual architectures. *Frontiers in neuroscience*, 13: 95.

Sennrich, R.; Haddow, B.; and Birch, A. 2015. Neural machine translation of rare words with subword units. *arXiv preprint arXiv:1508.07909*.

Shaw, P.; Uszkoreit, J.; and Vaswani, A. 2018. Self-attention with relative position representations. *arXiv preprint arXiv:1803.02155*.

Shazeer, N. 2020. Glu variants improve transformer. *arXiv preprint arXiv:2002.05202*.

Shoeybi, M.; Patwary, M.; Puri, R.; LeGresley, P.; Casper, J.; and Catanzaro, B. 2019. Megatron-lm: Training multi-billion parameter language models using model parallelism. *arXiv preprint arXiv:1909.08053*.

Smith, S.; Patwary, M.; Norick, B.; LeGresley, P.; Rajbhandari, S.; Casper, J.; Liu, Z.; Prabhumoye, S.; Zerveas, G.; Korthikanti, V.; et al. 2022. Using deepspeed and megatron to train megatron-turing nlg 530b, a large-scale generative language model. *arXiv preprint arXiv:2201.11990*.

Tan, M.; and Le, Q. 2019. EfficientNet: Rethinking Model Scaling for Convolutional Neural Networks. In Chaudhuri, K.; and Salakhutdinov, R., eds., *Proceedings of the 36th International Conference on Machine Learning*, volume 97 of *Proceedings of Machine Learning Research*, 6105–6114. PMLR.

Tavanaei, A.; Ghodrati, M.; Kheradpisheh, S. R.; Masquelier, T.; and Maida, A. 2019. Deep learning in spiking neural networks. *Neural networks*, 111: 47–63.

Tolstikhin, I. O.; Houlsby, N.; Kolesnikov, A.; Beyer, L.; Zhai, X.; Unterthiner, T.; Yung, J.; Steiner, A.; Keysers, D.; Uszkoreit, J.; et al. 2021. Mlp-mixer: An all-mlp architecture for vision. *Advances in Neural Information Processing Systems*, 34: 24261–24272.

Touvron, H.; Bojanowski, P.; Caron, M.; Cord, M.; El-Nouby, A.; Grave, E.; Izacard, G.; Joulin, A.; Synnaeve, G.; Verbeek, J.; et al. 2021a. Resmlp: Feedforward networks for image classification with data-efficient training. *arXiv preprint arXiv:2105.03404*.

Touvron, H.; Cord, M.; Douze, M.; Massa, F.; Sablayrolles, A.; and Jégou, H. 2021b. Training data-efficient image transformers & distillation through attention. In *International Conference on Machine Learning*, 10347–10357. PMLR.

Vaswani, A.; Shazeer, N.; Parmar, N.; Uszkoreit, J.; Jones, L.; Gomez, A. N.; Kaiser, Ł.; and Polosukhin, I. 2017. Attention is all you need. *Advances in neural information processing systems*, 30.

Wang, A.; Singh, A.; Michael, J.; Hill, F.; Levy, O.; and Bowman, S. R. 2018. GLUE: A multi-task benchmark and analysis platform for natural language understanding. *arXiv preprint arXiv:1804.07461*.

Wolf, T.; Debut, L.; Sanh, V.; Chaumond, J.; Delangue, C.; Moi, A.; Cistac, P.; Rault, T.; Louf, R.; Funtowicz, M.; Davison, J.; Shleifer, S.; von Platen, P.; Ma, C.; Jernite, Y.; Plu, J.; Xu, C.; Scao, T. L.; Gugger, S.; Drame, M.; Lhoest, Q.; and Rush, A. M. 2020. Transformers: State-of-the-Art Natural Language Processing. In *Proceedings of the 2020 Conference on Empirical Methods in Natural Language Processing: System Demonstrations*, 38–45. Online: Association for Computational Linguistics.

Wu, F.; Fan, A.; Baevski, A.; Dauphin, Y. N.; and Auli, M. 2019. Pay less attention with lightweight and dynamic convolutions. *arXiv preprint arXiv:1901.10430*.

Wu, K.; Peng, H.; Chen, M.; Fu, J.; and Chao, H. 2021. Rethinking and improving relative position encoding for vision transformer. In *Proceedings of the IEEE/CVF International Conference on Computer Vision*, 10033–10041.

Yang, J.; Li, C.; Zhang, P.; Dai, X.; Xiao, B.; Yuan, L.; and Gao, J. 2021. Focal self-attention for local-global interactions in vision transformers. *arXiv preprint arXiv:2107.00641*.

Yang, Z.; Dai, Z.; Yang, Y.; Carbonell, J.; Salakhutdinov, R. R.; and Le, Q. V. 2019. Xlnet: Generalized autoregressive pretraining for language understanding. *Advances in neural information processing systems*, 32.

Yin, B.; Corradi, F.; and Bohté, S. M. 2020. Effective and efficient computation with multiple-timescale spiking recurrent neural networks. In *International Conference on Neuromorphic Systems 2020*, 1–8.

Yun, S.; Han, D.; Oh, S. J.; Chun, S.; Choe, J.; and Yoo, Y. 2019. Cutmix: Regularization strategy to train strong classifiers with localizable features. In *Proceedings of the IEEE/CVF international conference on computer vision*, 6023–6032.

Zellers, R.; Bisk, Y.; Schwartz, R.; and Choi, Y. 2018. Swag: A large-scale adversarial dataset for grounded commonsense inference. *arXiv preprint arXiv:1808.05326*.

Zhang, H.; Cisse, M.; Dauphin, Y. N.; and Lopez-Paz, D. 2017. mixup: Beyond empirical risk minimization. *arXiv preprint arXiv:1710.09412*.

Zhong, Z.; Zheng, L.; Kang, G.; Li, S.; and Yang, Y. 2020. Random erasing data augmentation. In *Proceedings of the AAAI conference on artificial intelligence*, volume 34, 13001–13008.

A Appendix

A.1 Explanation Of Gate With Inhibition

Shunting Inhibition (Gate With Inhibition): The architecture of Gate With Inhibition is inspired from shunting inhibition mechanism (Borg-Graham, Monier, and Fregnac 1998; Huang et al. 2021). In Figure 4, the left panel presents the working of shunting inhibition with its on (the red box) and off (the green box) states. If the gate of the shunting inhibition is off, the transmission will transport across the joint which can be influenced by shunting synapses. The shunting synapse plays an important role on gating the function of neurons, and its switch will influence the receive and the send of signals. In artificial neural networks (ANNs), the

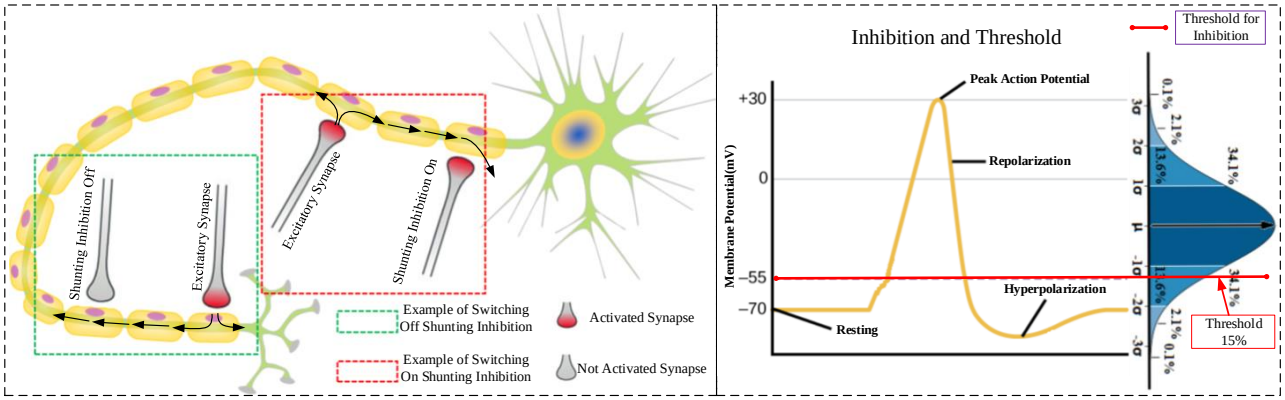

Figure 4: Inspiration from Neuroscience: Gate With Inhibition.

shunting can be described and presented as gating in most articles, but researchers forgot and ignored the inhibition mechanism during these decades. Shunting Inhibition used the shunting mechanism to select the activated neuron units, and the direct and obvious function is to select, weaken or enforce quantized features in ANNs.

In contrast to excitatory synapses, some neurotransmitter-gated ion channels can drive the postsynaptic potential towards the resting potential or inhibit the effect of excitatory synapses (Borg-Graham, Monier, and Fregnac 1998). Such synapses are collectively called inhibitory. A prominent example of inhibitory synapses uses the neurotransmitter $GABA$ with a fast receptor called $GABA_A$ and a slower receptor called $GABA_B$. The neurotransmitter Dopamine has several receptor types, some of which are excitatory and some of which are inhibitory. Inhibition can be subtractive in the sense that it lowers the membrane potential. However, inhibition can also be divisive in the sense that it modulates the effect of excitation. For example, $GABA_A$ receptors have no effect on the membrane potential if the membrane potential is at rest, so it does not reduce the potential further. Inhibitory synapses close to the cell body can have such modulatory (multiplicative) effects on summed excitatory postsynaptic potentials (EPSPs).

Membrane Potentials and Threshold: In Figure 4, the right panel shows the reason why we should set the threshold between 10% and 30%. The red line is the threshold for inhibition, and the approximate range of membrane potentials is from $-70mV$ to $+30mV$. After considering the inactivated range of membrane potentials, we roughly set the threshold as 15% (a number from 10% to 30%), as not all neurons can act as such and have the 15% threshold. If the voltage is greater than the threshold, the depolarization would be executed following the activation. We assume that the distribution of activated features in artificial neural networks is a Gaussian like type. Mostly used activation functions, for example, Softmax, Tanh, ReLU (Agarap 2018), Parametrized ReLU (He et al. 2015), ELU (Clevert, Unterthiner, and Hochreiter 2015), Switsh (Ramachandran, Zoph, and Le 2017), GELU (Hendrycks and Gimpel 2016), SELU (Klambauer et al. 2017), choose to directly activate features without a further selection. To avoid the inference of unimportant features, the features whose activated values are below the threshold should be inhibited. These features have no significance on some specific tasks, as the pretrained model can provide huge quantized features for fine-tuning tasks.

A.2 Image Classification Implementation Details

Settings. We train our models on the ImageNet-1K dataset (Deng et al. 2009), which contains 1.2M training images and 50K validation images evenly spreading 1,000 categories. We follow the standard practice in the community by reporting the top-1 accuracy on the validation set. Our code is implemented based on PyTorch (Paszke et al. 2019) framework and heavily relies on the timm repository. For apple-to-apple comparison, our training strategy is mostly adopted from DeiT (Touvron et al. 2021b), which includes RandAugment (Cubuk et al. 2020), Mixup (Zhang et al. 2017), Cutmix (Yun et al. 2019) random erasing (Zhong et al. 2020) and stochastic depth (Huang et al. 2016). The optimizer is AdamW (Loshchilov and Hutter 2017) with the momentum of 0.9 and weight decay of by default. The cosine learning rate schedule is adopted with the initial value of. All models are trained for 300 epochs on 8 Tesla V100 GPUs with a total batch size of 1024.

Algorithm 1: Pseudo-Code of giMLPs Block

Input: X, Inh_p.

set shortcut:
$L_{w,bias}$=$GELU(proj(X, W, axis = "channel"))$;

gate layer:
$L_g = GELU(proj(X, W_g, axis = "channel"))$;

set inhibition:
$L_g = GELU(L_g - max(L_g) \times Inh_p)$;

inhibition layer:
$L_i = GELU(proj(L_g, W_i, axis = "channel"))$;

output of giMLP: $Z_{gi} = L_{gi} + L_{w,bias}$;

return Z_{gi};

Output: Z_{gi}

Our code is implemented based on DieT (Touvron et al. 2021b) [1] and CyclePLM (Chen et al. 2022) [2].

A.3 Language Modeling Implementation Details

Settings. Following BERT (Devlin et al. 2018), RoBERTa (Liu et al. 2019), DeBERTa (He et al. 2020), we adopt dynamic data batching. We also include span masking (Joshi et al. 2020) as an additional masking strategy with the span size up to three. We list the detailed hyperparameters of pretraining in Table 8. For fine-tuning, we use Adam (Kingma and Ba 2014) as the optimizer for a fair comparison. For fine-tuning, we train each task with a hyper-parameter search procedure, each run takes about 1-2 hours on a DGX-2 node. All the hyper-parameters are presented in Table 9. The model selection is sbased on the performance on the task-specific development sets.

Algorithm 2: Pseudo-Code of giTransformers Block

Input: H, Inh_p.

set Value: V=$GELU(proj(H, W_v, axis = "channel"))$;

set shortcut on Key: K=$GELU(proj(H, W_k, axis = "channel"))$;

set shortcut on Query: Q=$GELU(proj(H, W_q, axis = "channel"))$;

gate layer on Key Side: $G_k = GELU(proj(H, W_{kg}, axis = "channel"))$;

gate layer on Query Side: $G_q = GELU(proj(H, W_{qg}, axis = "channel"))$;

set inhibition on Key Side: $G_k = G_k - max(G_k) \times Inh_p$;

set inhibition on Query Side: $G_q = G_q - max(G_q) \times Inh_p$;

inhibition layer on Key Side: $I_k = GELU(proj(G_k, W_{ki}, axis = "channel"))$;

inhibition layer on Query Side: $I_q = GELU(proj(G_q, W_{qi}, axis = "channel"))$;

get gated Key with inhibition: $B_k = I_k + K$;

get gated Key with inhibition: $B_q = I_q + Q$;

activation of attention: $\bar{A}_{kq} = \frac{B_q B_k^T}{\sqrt{d}}$;

output of giTranformers: $\bar{H}_o = softmax(\bar{A}_{kq})V$;

return $\bar{H}_o$;

Output: $\bar{H}_o$

Our code is implemented based on Huggingface Transformers (Wolf et al. 2020) [3]. Our experience is during fine-tuning on downstream tasks, firstly we set the inhibition percentile as 90%, if the result is similar to the settings without Gate With Inhibition, and then, we set the inhibition percentile as 10% or 30%.

A.4 Ablation: Gate MLPs With Inhibition

Notation. We denote an input feature map as $X \in R^{M_1 \times M_2 \times D}$, where M_1, M_2 denote the height and width of the image and D is the number of feature channels. $W, W_g, W_i \in R^{M \times M}$ are matrices for whose size is the same as the sequence length, $bias, bias_g, bias_i \in R^{1 \times D}$ refer biases. See Appendix Algorithm1.

Motivation. The motivation behind giMLPs is to assemble a flexible gate with an adjustable quantized inhibition to cope with downstream dense prediction tasks while maintaining the important features and inhibiting nonsignificant features. As illustrated in the left panel of Figure2, the right branch is a gate with inhibition block, which applies a SGU with an adjustable threshold on gating excited layers. We formulate the linear gate with inhibition block in CNNs as:

$$L_{w,bias}(X) = WX + bias \tag{14}$$

$$L_{gi}(X) = GELU\{W_i[GELU(W_g X + bias_g)] + bias_i - Th\} \tag{15}$$

$$Z_{gi}(X) = L_{gi} L_{w,bias}(X) + L_{w,bias}(X) \tag{16}$$

where $L_{gi}(X)$ is the projection of gate with inhibition layers, and $Z_{gi}(X)$ is the output of linear gating with inhibition. Th is the product of $max(W_i[GELU(W_g X + bias_g)]) \times Inh_p$.

In this section, we report the results of one MLP family CNN - CycleMLP (Chen et al. 2022) - on ImageNet with different inhibition percentiles. Following and comparing with previous CycleMLP (Chen et al. 2022), we use 8 $\times$ NVIDIA Tesla V100 with 32GB graphic memory to train the models. A single model trained with 1024 batch size and 300 epochs takes about 21 days. Refer to Appendix A.2 Table 2 for the detailed hyperparamters. We summarize the result on Table 4.

We examine giMLP in the vision domain, and apply ImageNet (Deng et al. 2009) without using extra data on image classification task. We compare our giMLP model with recent MLP-like models, including ResMLP (Touvron et al. 2021a), gMLP (Liu et al. 2021b) and CycleMLP (Chen et al. 2022), as well as several other representative convolutional networks. For the capacity of comparing, models should choose the depth and width according to the same size.

Our giMLP has the natural inhibition capacity, which can inhibit the feature selection in the gating branches of neural networks trunk. Although the final result of giCycleMLP with threshold 10% on ImageNet classification task cannot surpass the original CycleMLP, the gap between them can be ignored after training over 100 epochs. This acceptable gap 0.1% verifies that the gating MLP architecture with inhibition can produce the equal performance without inhibition inside the gating MLP. In Figure 5(a), the accuracy curves show that the gap between with and without inhibition mechanism is

[1] https://github.com/facebookresearch/deit

[2] https://github.com/ShoufaChen/CycleMLP

[3] https://github.com/huggingface/transformers

Table 2: Hyper-parameters for Image classification on ImageNet-1K with Gate With Inhibition mechanism.

Hyper-parameter	**Cycle+giMLP-B1 threshold(0%)**	**Cycle+giMLP-B1 threshold(10%)**	**Cycle+giMLP-B1 threshold(30%)**	**Cycle+giMLP-B1 threshold(90%)**
Data augmentation	AutoAugment			
Repeated Augmentation	off			
Input resolution	224			
Epochs	300			
Batch size	1024			
Warmup steps	10K			
Hidden dropout	0			
GELU dropout	0			
Attention dropout (if applicable)	0			
Classification dropout	0			
Random erasing prob	0			
EMA decay	0			
Cutmix α	1.0			
Mixup α	0.8			
Cutmix-Mixup switch prob	0.5			
Label smoothing	0.1			
Peak learning rate	1e-3			
Learning rate decay	cosine			
Optimizer	AdamW			
Adam ϵ	1e-6			
Adam (β_1, β_2)	(0.9, 0.999)			
Weight decay	0.05			
Gradient clipping	1.0			
Inhibition Percentile	0.0	0.1	0.3	0.9

Table 3: Hyper-parameters for fine-tuning BERT, RoBERTa and DeBERTa with Gate With Inhibition mechanism on downstreaming tasks.

Hyper-parameter	**BERT**(large)	**RoBERTa**(large)	**DeBERTa**(large)
Dropout of task layer	0.15	0.15	0.15
Warmup Steps	100	100	100
Learning Rates	5e-6	5e-6	5e-6
Batch Size	{16,32,64}	{16,32,64}	{16,32,64}
Weight Decay	0.01	0.01	0.01
Maximum Training Epochs	5	10	10
Learning Rate Decay	Linear	Linear	Linear
Optimizer	AdamW	AdamW	AdamW
Adam ϵ	1e-6	1e-6	1e-6
Adam (β_1, β_2)	(0.9, 0.999)	(0.9, 0.999)	(0.9, 0.999)
Gradient Clipping	1.0	1.0	1.0
Inhibition Percentile	(0.0, 0.1, 0.3, 0.9)	(0.0, 0.1, 0.3, 0.9)	(0.0, 0.1, 0.3, 0.9)

Table 4: Comparison with SOTA models on ImageNet-1K without an extra data.(Note that missing results in literature are signified by "-").

Model	**Family**	**Para**	**FLPOs**	**Scale**	**Top-1**
EffNet-B3(Tan and Le 2019)	CNN	12M	1.8G	300	81.6
GFNet-H-Ti(Rao et al. 2021)	FFT	15M	2.0G	224	80.1
ResMLP-S12(Touvron et al. 2021a)	MLP	15M	3.0G	224	76.6
gMLP-S(Liu et al. 2021b)	MLP	20M	4.5G	224	79.6
CycleMLP-B1(Chen et al. 2022)	MLP	15M	2.1G	224	78.9
Cycle+**gi**MLP-B1 (thre=0%)	MLP	15M	2.1G	224	78.9
Cycle+**gi**MLP-B1 (thre=10%)	MLP	15M	2.1G	224	78.8
Cycle+**gi**MLP-B1 (thre=30%)	MLP	15M	2.1G	224	76.6
Cycle+**gi**MLP-B1 (thre=90%)	MLP	15M	2.1G	224	-

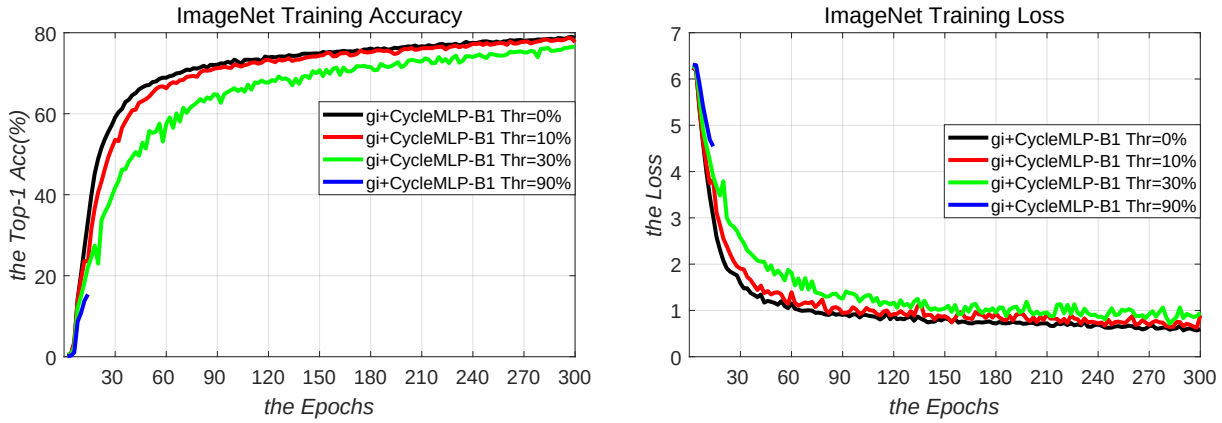

(a) Cycle+giMLPs-B1 Test Curve on ImageNet

(b) Cycle+giMLPs-B1 Loss Curve on ImageNet

Figure 5: Plots of (a) top1 accuracy and (b) loss according to the number of epochs on the train split of ImageNet.

shrinking during training, and all final results tend to reach the same level. Although from 10-epoch to 50-epoch when setting inhibition percentile as 10%, to a great extent, the giCycleMLP inhabit the branch gating function because of the natural inhibition capacity of giCycleMLP, but after that, the giCycleMLP will catch up the original CycleMLP in over 120 epoches. Excessive inhibition in gating MLP needs more training steps to adjust and regain equalizer. Gate with inhibition embedded in MLPs, in general, will play an gating inhibition role on selecting branch features. But it is not similar to the sparsity of CNNs which will totally abandon randomly selected vectors or set zeros on them, our gate with inhibition will attach a negative value on those unimportant features, not remove or set zeros on them, especially after the activation of GeLU or LeakyReLU, whose tails can provide negative values.

A.5 Ablation: The Influence Of Different Activation Functions On Gating With Inhibition

Because of the short negative tail of GELU, we specifically select it as the activation function. Although LeakyReLU also has a long negative tail, the negative value after LeakyReLU activation of negative features would provide a huge inhibition for BERT or relatives of BERT (RoBERTa, DeBERTa and DeBERTaV3). We summarize the results of using different activation functions after setting inhibition percentile as 30% in Table 5. Compared to activation functions whose tails are zero or big negative values, the GELU activation function whose negative tail are short achieves best improvement on QQP, SST-2, QNLI, MRPC and GLUE average. Although LeakyReLU with default slope gets outstanding performance on CoLA and RTE, the total effect on GLUE tasks is inferior to GELU. LeakyReLU can provide more stable and smooth negative values, and this would be the reason why LeakyReLU can putperform GELU on these two small downstream GLUE tasks.

A.6 Ablation: The Gate With Inhibition In Single Side

We denote input hidden vectors as $H \in R^{M\times D}$ and the output of self-attention as $\bar{H}_o \in R^{M\times D}$. $W_{kg}, W_{ki}, W_{qg}, W_{qi}, W_v \in R^{M\times D}$ are the projection matrices. M is the length of the input sequence and D is the dimension of hidden states. We summarize the result on Table 6.

The Gate With Inhibition In Key Side. We formulate the linear gate with inhibition layer in Transformers' Key side as:

$$G_k = GELU(HW_{kg} + bias_{kg}) \tag{17}$$

$$I_k = GELU(G_k W_{ki} + bias_{ki} - Th_k) \tag{18}$$

$$V = HW_v + bias_v, K = HW_k + bias_k, Q = HW_q + bias_q \tag{19}$$

$$B_k = K + I_k, \bar{A}_k = \frac{QB_k^T}{\sqrt{d}} \tag{20}$$

$$\bar{H}_o = softmax(\bar{A}_k + bias_{\bar{a}})V \tag{21}$$

where $G_k, I_k \in R^{M\times D}$ are the $Gate$ and $Inhibition$ matrices in Key side, and $V \in R^{M\times D}$ is the $Value$ matrix. $B_k \in R^{M\times D}$ is Key matrices with Gate With Inhibition. $\bar{A}_k \in R^{M\times D}$ is the attention matrix with Gate With Inhibition. $bias_{kg}, bias_{ki}, bias_v, bias_{\bar{a}} \in R^{M\times M}$ are the relative position bias term for each head. Th_k is the product of $max(G_k W_{ki}) \times percentile$.

The Gate With Inhibition In Query Side. We formulate the linear gate with inhibition layer in Transformers' Query side as:

Table 5: Comparison results on the GLUE development set with five epochs fine-tuning based on BERT. (Note that missing results in literature are signified by "-").

	GLUE								
Model-large	CoLA	QQP	MNLI-m/mm	SST-2	STS-B	QNLI	RTE	MRPC	
#Train	Mcc	Acc	Acc	Acc	Corr	Acc	Acc	Acc	Avg.
gi+BERT(thre=30%)	8.5k	364k	393k	67k	7k	108k	2.5k	3.7k	
GELU(Hendrycks and Gimpel 2016)	65.9	***91.5***	86.3/-	***94.4***	89.0	***92.7***	69.0	***84.8***	***84.20***
SELU(Klambauer et al. 2017)	62.1	63.2	35.4/-	50.9	32.0	50.5	54.9	68.4	44.41
ELU(Clevert, Unterthiner, and Hochreiter 2015)	62.8	63.2	35.5/-	92.9	77.0	92.0	52.7	77.2	69.15
LeakyReLU(He et al. 2015)	***66.6***	91.4	86.3/-	93.6	88.9	92.3	***70.0***	84.3	84.18
ReLU(Agarap 2018)	64.3	91.4	86.3/-	93.1	***89.3***	92.3	68.6	83.8	83.64

Table 6: Comparison results on fine-tuning the GLUE development set, SQuAD v1.1, SQuAD v2.0, SWAG and NER. (Note that **Key*** and **Query*** respectively mean the gate with inhibition in Transformers' Key side and Query side).

	Model	**GLUE**									**SQuAD v1.0**	**SQuAD v2.0**	**SWAG**	**NER**
	(Large)	CoLA	QQP	MNLI-m/mm	SST-2	STS-B	QNLI	RTE	MRPC	Avg.	F1/EM	F1/EM	Acc	F1
	#Train	Mcc	Acc	Acc	Acc	Corr	Acc	Acc	Acc		87.6k	130.3k	73.5k	14987
		8.5k	364k	393k	67k	7k	108k	2.5k	3.7k					
Key*	giDeBERTaV3(0)	72.6	93.0	90.9/90.9	96.3	92.8	95.4	88.8	92.2	90.25	94.8/89.2	89.9/86.5	92.2	96.8
	giDeBERTaV3(0.1)	74.0	93.0	91.2/91.0	96.2	92.9	95.4	89.5	91.9	90.51	94.8/89.3	89.7/86.9	91.6	96.8
	giDeBERTaV3(0.3)	75.0	93.1	91.0/90.9	96.2	92.8	95.3	91.7	91.7	90.85	95.8/89.3	89.9/86.4	92.2	96.8
	giDeBERTaV3(0.9)	72.0	93.1	91.0/91.0	96.3	92.8	95.4	91.3	91.4	90.41	94.8/89.3	90.3/86.9	92.0	96.5
Query*	giDeBERTaV3(0)	71.9	93.0	91.0/90.9	96.2	92.8	95.3	**92.1**	90.2	90.31	94.7/89.2	90.1/86.9	92.2	96.5
	giDeBERTaV3(0.1)	73.2	92.9	91.3/90.9	96.3	92.7	95.1	89.2	90.2	90.11	95.8/89.5	90.4/87.7	92.2	96.8
	giDeBERTaV3(0.3)	73.5	92.9	91.3/90.9	96.2	93.0	95.4	89.5	91.9	90.46	94.8/89.3	89.7/86.9	91.6	97.3
	giDeBERTaV3(0.9)	74.2	93.0	90.8/90.8	95.6	92.9	95.4	90.6	90.2	90.34	94.8/89.5	89.8/86.7	92.0	96.6

$$G_q = GELU(HW_{qg} + bias_{qg}) \tag{22}$$

$$I_q = GELU(G_q W_{qi} + bias_{qi} - Th_q) \tag{23}$$

$$V = HW_v + bias_v, K = HW_k + bias_k, Q = HW_q + bias_q \tag{24}$$

$$B_q = Q + I_q, \bar{A}_q = \frac{B_q K^T}{\sqrt{d}} \tag{25}$$

$$\bar{H}_o = softmax(\bar{A}_q + bias_{\bar{a}})V \tag{26}$$

where $G_q, I_q \in R^{M\times D}$ are the $Gate$ and $Inhibition$ matrices in $Query$ side, and $V \in R^{M\times D}$ is the $Value$ matrix. $B_q \in R^{M\times D}$ is $Query$ matrices with Gate With Inhibition. $\bar{A}_q \in R^{M\times D}$ is the attention matrix with Gate With Inhibition. $bias_{qg}, bias_{qi}, bias_v, bias_{\bar{a}} \in R^{M\times M}$ are the relative position bias term for each head. Th_q is the product of $max(G_q W_{qi}) \times Inh_p$.

For the single side conditions, both the Key side and the Query side, they show the trend same as the two side condition. When the inhibition level is 30%, we get the best GLUE average score under using both Key side and Query side. There is an unexpected finding that when using the gate with 0% inhibition level, fine-tuning the downstream RTE task can achieve the best result at 92.1%.